Pharm Res (2014) 31:35–45
DOI 10.1007/s11095-013-1127-z

RESEARCH PAPER

Dual Physiologically Based Pharmacokinetic Model of Liposomal and Nonliposomal Amphotericin B Disposition

Leonid Kagan • Pavel Gershkovich • Kishor M. Wasan • Donald E. Mager

Received: 16 April 2013 / Accepted: 14 June 2013 / Published online: 21 June 2013

ABSTRACT

Purpose To investigate the biodistribution of amphotericin B (AmB) in mice and rats following administration of liposomal AmB (AmBisome®) using a physiologically-based pharmacokinetic (PBPK) modeling framework and to utilize this approach for predicting AmBisome® pharmacokinetics in human tissues.

Methods AmB plasma and tissue concentration-time data, following single and multiple intravenous administration of nonliposomal and liposomal AmB to mice and rats, were extracted from literature. The whole-body PBPK model was constructed and incorporated nonliposomal and liposomal subcompartments. Various structural models for individual organs were evaluated. Allometric relationships were incorporated into the model to scale parameters based on species body weight.

Results A non-Michaelis-Menten mechanism was included into the structure of the liver and spleen liposomal compartments to describe saturable uptake of particles by the reticuloendothelial system. The model successfully described plasma and tissue pharmacokinetics of AmB after administration of AmBisome® to rats and mice.

Conclusions The dual PBPK model demonstrated good predictive performance by reasonably simulating AmB exposure in human tissues. This modeling framework can be potentially utilized for optimizing AmBisome® therapy in humans and for investigating pathophysiological factors controlling AmB pharmacokinetics and pharmacodynamics.

KEY WORDS amphotericin B · interspecies scaling · physiologically-based pharmacokinetic model · tissue distribution

INTRODUCTION

Amphotericin B (AmB) is an important pharmacological agent for the treatment of severe fungal and parasitic infections. The conventional deoxycholate micellar formulation (Fungizone®) can be associated with serious adverse reactions (e.g., nephrotoxicity), which limits the available range of dose levels and the duration of therapy. Several lipid-based particulate formulations of AmB have been developed (e.g., liposomal AmBisome® and lipid-complex Abelect®). These formulations exhibit lower toxicity and comparable efficacy to that of Fungizone® and hence currently prevail in clinical use in developed countries. However, high cost associated with lipid-based formulations of AmB limit their use in developing countries (1,2).

AmBisome® is composed of hydrogenated soy phosphatidylcholine, distearoyl phosphatidylglycerol and cholesterol. AmB is strongly associated with the bilayer structure of small rigid unilamellar liposomes with a mean diameter of less than 100 nm (3). This particulate nature of AmBisome® makes it especially attractive for treating diseases associated with the reticuloendothelial system (RES), such as visceral leishmaniasis (4). Due to its amphiphilic properties (Biopharmaceutical Classification System class IV compound (5)) the oral bioavailability

Electronic supplementary material The online version of this article (doi:10.1007/s11095-013-1127-z) contains supplementary material, which is available to authorized users.

L. Kagan (✉)
Department of Pharmaceutics, Ernest Mario School of Pharmacy
Rutgers, The State University of New Jersey, 160 Frelinghuysen Rd.
Piscataway, New Jersey 08854, USA
e-mail: lkagan@pharmacy.rutgers.edu

P. Gershkovich
School of Pharmacy, The University of Nottingham, Nottingham, UK

K. M. Wasan
Faculty of Pharmaceutical Sciences, The University of British Columbia, Vancouver, Canada

D. E. Mager
Department of Pharmaceutical Sciences, University at Buffalo, The State University of New York, Buffalo, USA

of commercially available AmB formulations is negligible and AmB has to be administered intravenously to achieve systemic exposure.

The pharmacokinetic behavior of particulate formulations of drugs can be substantially different from that of the free or unmodified drug (6–8). These changes arise from alterations in drug clearance and tissue distribution patterns. The differences among lipid-based formulations are dependent on the uptake of particles by macrophage cells in the organs of the RES (i.e., liver, spleen, bone marrow, lungs). Particle recognition, uptake rate, and tissue capacity are dependent on multiple factors, including particle size, composition, surface properties, and dose (9,10), as well as species-related differences (11,12). Moreover, disease states that affect the organs of the RES (such as visceral leishmaniasis) can alter the uptake of particulate formulations into target organs, which can potentially attenuate treatment efficacy (13). Overall drug disposition likely reflects a combination of properties of the drug associated with particles, as well as released drug.

AmB exhibits multiple pharmacokinetic complexities that impede the understanding of exposure-response relationships for this compound. No correlation between plasma concentration and clinical effect has been established (14,15) most probably due to its extensive tissue distribution and prolonged tissue half-lives. The advantage of physiologically-based pharmacokinetic (PBPK) models is their mechanistic description of drug disposition that provides a platform for scaling pharmacokinetics between species and ultimately for predicting the exposure of compounds in humans (16). We have previously developed a PBPK model for the pharmacokinetics of AmB in rats after intravenous administration of a micellar deoxycholate formulation (Fungizone®) (17). The model provided a good simultaneous description of plasma and tissue (liver, spleen, kidneys, heart, lungs, and gut) distribution of AmB following single or multiple dose regimens in rats. The differences in half-life in various tissues were captured by applying several structural models for each organ. Furthermore, the model was qualified through reasonable predictions of plasma concentration-time profiles of AmB in mice and humans for intravenous bolus injections. Quantification of nonliposomal AmB biodisposition is an important prerequisite toward understanding the pharmacokinetics of particulate formulations. The purpose of this work is to investigate the biodistribution of AmB in mice and rats following administration of liposomal AmB (AmBisome®) using a PBPK modeling framework and to adopt this approach for predicting AmBisome® pharmacokinetics in human tissues.

MATERIALS AND METHODS

Data Sources

Literature reports containing plasma and/or tissue concentration-time profiles of AmB following administration of Fungizone® and AmBisome® to mice, rats, and humans were identified (Table I). Mean data were captured by computer digitization or extracted from tables. The PBPK model structure for nonliposomal AmB does not contain nonlinear processes (17); therefore, for simplicity, the data for Fungizone® in mice were normalized to a 1 mg/kg dose level. For rats and humans, total and nonliposomal concentration-time profiles were available after single IV dosing of AmBisome®. The majority of the tissue data were available for mice only (Table I).

Physiological parameters, such as tissue weights, fractions of vascular space in tissues, and plasma flow rates to select organs, were fixed to literature values (Supplementary Material Table S1) (18–21). Mean body weights of 24 gr, 250 gr, and 70 kg were assumed for mice, rats, and humans. Plasma cardiac output (CO) for rats and mice was calculated using allometric relationships: CO_{rat} (L/h) = 14.1 · (1 - Hematocrit) · (Body weight in kg)$^{0.75}$ and CO_{mouse} (L/h) = 16.5 · (1-Hematocrit) · (Body weight in kg)$^{0.75}$. Cardiac output for humans (70 kg) was fixed to 312 L/h (18). All tissues that were not available were lumped into a remainder compartment (22). Fraction unbound in plasma (f_u^{pl}) for mice, rats, and humans were fixed to 0.074, 0.11, and 0.052 (23). A density of 1 was assumed for all tissues (17). Clearance mechanisms for nonliposomal AmB included renal and biliary elimination (24–26). No metabolic pathway has been identified for AmB (27).

Model Development

AmB Release Model

No *in vitro* data were available for AmB release kinetics from liposomes. For initial evaluation of the release rate of AmB from liposomes, plasma concentration-time profiles for total and nonliposomal drug following administration of AmBisome® and nonliposomal drug following administration of Fungizone® to rats and humans were used. It was hypothesized that following Fungizone® intravenous injection, the concentration of the formulation falls rapidly below the critical micelle concentration (CMC), and AmB pharmacokinetics is mainly driven by the properties of the drug molecule itself (17) (the concentration of deoxycholate in Fungizone® infusion solution is approximately 0.2 mM, and the reported CMC is 2–6 mM). The pharmacokinetic parameters of AmB after injection of Fungizone® were estimated by fitting a classical two-compartment model with linear elimination (Supplementary Material Figure S1). These parameters were assumed to represent the parameters for the nonliposomal AmB and were fixed. The disposition of liposomal AmB was assumed to follow two-compartment model with linear elimination and a first-order release process from the liposomal compartments to the corresponding nonliposomal compartments (Supplementary Material Figure S1). The model fit was performed separately for rat and human data. The base

Table I Sources of AmB Pharmacokinetic Data

Species	AmB formulation	Dosing regimen	Assay	Reference
Mouse	Fungizone	2 mg/kg q24h for 5 days	HPLC-UV	(42)
Mouse	Fungizone	0.3 mg/kg	HPLC-UV	(41)
Rat	Fungizone	0.8 mg/kg	HPLC-UV	(6)
Human	Fungizone	0.6 mg/kg 2 h infusion	LC/MS/MS	(43)
Rat	AmBisome	20 mg/kg	HPLC-UV	(27)
Mouse	AmBisome	5 mg/kg	HPLC-UV	(44)
Mouse	AmBisome	15 mg/kg × 3/week for 5 weeks	Bioassay	(45)
Mouse	AmBisome	2 mg/kg	HPLC-UV	(13)
Human	AmBisome	2 mg/kg 2 h infusion	LC/MS/MS	(24)

HPLC-UV—high performance liquid chromatography with UV absorbance detector; LC/MS/MS—liquid chromatography with tandem mass spectrometry detector

model could not describe the concentration-time profiles satisfactorily, and incorporation of an additional parameter (*FR*, fraction of the dose that undergoes rapid release) was required for capturing the data in both species. The final values of the release rate constant (0.0035 h^{-1}) and immediate release fraction (1.83% for rats and 8.16% for humans) estimated by this model were incorporated into the PBPK model.

Nonliposomal PBPK Model

The nonliposomal PBPK model framework (including structures of individual organs and parameters values) for biodistribution of nonliposomal AmB was adopted from a previous model (Fig. 1, compartments with grey background) (17). Briefly, the whole-body PBPK model was constructed and included liver, spleen, kidneys, gut, lungs, and heart compartments. All other tissues were lumped into a remainder compartment. These compartments were arranged in anatomical order and connected through a plasma compartment. The structure of individual organs included one, two, or three subcompartments. The distribution of AmB to tissue was govern by a partition coefficient (*Kpti* for liver, heart, lung, and gastro-intestinal tract); permeability-surface area term (PS_{ti}) and tissue unbound fraction (f_u^{ti}) (remainder compartment); or PS_{ti}, f_u^{ti}, and distribution rate constants to and from a "deep tissue" subcompartment (k_a and k_d, spleen and kidneys). Clearance terms were assigned to the liver (Cl_{li}) and kidney (Cl_{kd}) compartments, reflecting biliary and urinary excretion of AmB (24–26). Another clearance term was incorporated into the remainder compartment (Cl_{rm}) to account for an additional elimination pathway, as previously described (17). All parameters for the nonliposomal AmB were fixed to the values estimated in a previous study (Online supplement, Table S3), with the exception of partition coefficient for lung tissue.

Interspecies Scaling

An approach for scaling model parameters for nonliposomal model has been described previously (17). Briefly, species-specific physiological parameters and f_u^{pl} values were used,

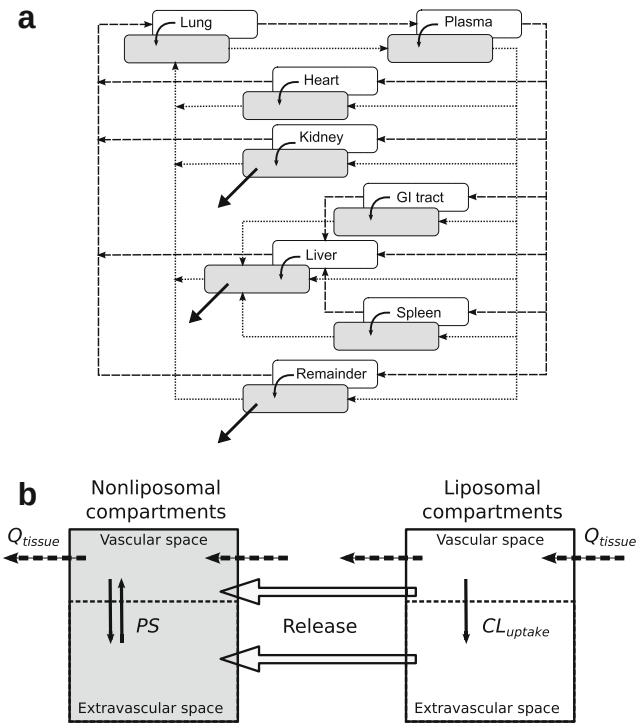

Fig. 1 Schematic of the dual PBPK model of AmB in mice, rats, and humans after intravenous injection of AmBisome® and Fungizone®. (**a**) Whole-body model. (**b**) Structure of a tissue subcompartments. Q_{tissue} plasma flow rate to the organ; Cl_{uptake} uptake of liposome into the tissue, *PS* permeability-surface area coefficient that governs tissue distribution of nonliposomal AmB.

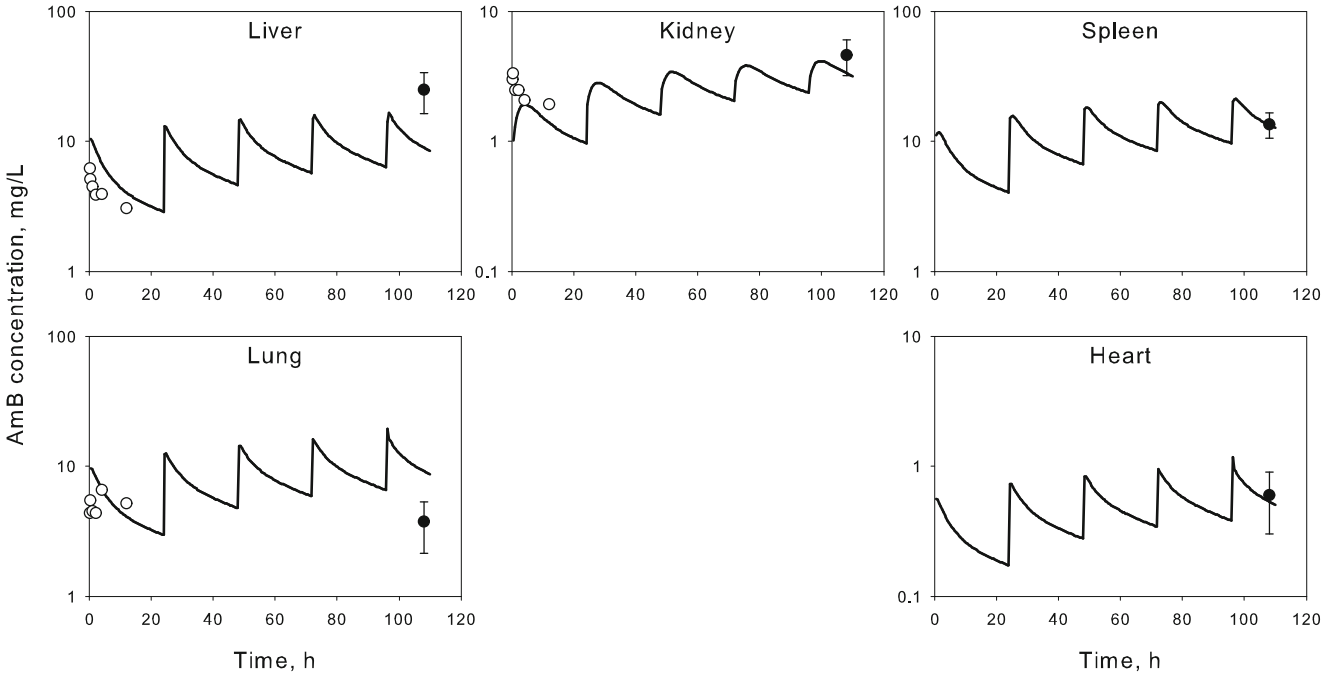

Fig. 2 Time-course of AmB in different tissues of mice following single and multiple IV bolus administration of Fungizone. *Symbols* represent data extracted from references (○—single dose (41) and ●—multiple dose (25,42)), and lines are PBPK model predicted profiles using the model structure from (17). Profiles were normalized for 1 mg/kg dose. *Error bars* represent S.D. (where available).

whereas Kp_{ti}, f_u^{ti}, ka_{ti} and kd_{ti} were assumed to be identical among the species. Cl_{ti} and PS_{ti} were predicted from the values estimated for rats using an allometric equation:

$$P = P_{rat}\left(\frac{BW}{BW_{rat}}\right)^{b} \quad (1)$$

where P is the parameter of interest, BW is species body weight, and b is an allometric exponent (fixed to 0.75 for renal and biliary clearances). For Cl_{rm} the value of b was fixed to 1. It was assumed that permeability of tissues for AmB is similar and that accessible surface area is proportional to $BW^{0.67}$. Thus, the value of b was fixed to 0.67 for PS_{ti} (28). For liposomal compartments, the values for uptake clearance ($Upti$) were scaled with body weight (Eq. 1), where different values of b were evaluated and mouse parameters were used as the reference species. The release rate of AmB, fraction of immediate release and maximal liposomal tissue concentrations in spleen and liver were kept constant.

Modeling Strategy

The rat PBPK model for Fungizone® was previously used to predict plasma profiles of AmB in mice and humans by scaling rat model parameters (17). The first phase of the present analysis included evaluating the ability of this model to predict tissue AmB concentration-time profiles in mice and characterizing AmB release from liposomes using the compartmental release model (Online supplement, Figure S1). For the next phase, the dual PBPK model was constructed (Fig. 1). AmB pharmacokinetics following AmBisome® administration was assumed to be comprised of liposomal and nonliposomal drug disposition. Liposomal AmB circulates through tissues *via* blood capillaries and can undergo release to its nonliposomal form by a first-order rate constant (r_{el}). The release was assumed to occur in both plasma and tissue spaces. Previous studies in humans suggest that renal and biliary elimination of AmB occurs following the release of the drug from liposomes (24); therefore, a separate elimination pathway for liposomal AmB was not included in the model. The disposition and elimination of the released drug was assumed to follow the model developed for Fungizone®. For liposomal distribution, each tissue compartment was divided into two subcompartments (vascular and extravascular), with a unidirectional uptake process (Up_{ti}). The whole body PBPK model was fit simultaneously to mouse and rat data, and the pertinent parameters were estimated. Initially, a linear uptake mechanism was assumed for all tissues; however, this model did not accurately describe the data. A saturable uptake mechanism driven by the concentration of the drug within the tissue (C_{ti}^{MAX}) was added to the structure of the spleen and liver liposomal compartments (29,30). The equations used to define the dual PBPK model are shown in the Supplementary Material.

During the final analysis phase, the ability of the dual PBPK model to predict biodisposition of AmB in humans following single IV administration of AmBisome® was evaluated *via* simulations. Human physiological parameters were utilized. Liposomal and nonliposomal plasma drug concentrations following

administration of AmBisome® to humans were simulated and visually compared to data available in the literature. In addition, simulations were performed to generate concentration-time profiles of AmB in various tissues following multiple-dosing of AmBisome®. The resulting profiles were overlaid with limited tissue sample data from autopsy reports (31,32). Although the exact dosing schedules and sampling times were not reported for these studies, a daily dose of 2.2 mg/kg was used, which is in agreement with the median daily dose reported in these case studies.

Data Analysis

Modeling and simulations were performed using MATLAB R2008a (The MathWorks, Natick, MA). All parameters were estimated using maximum likelihood, and the variance model was defined as: $VAR_i=(\sigma_1+\sigma_2\cdot Y(\theta,t_i))^2$, where VAR_i is the variance of the *ith* data point, σ_1 and σ_2 are the variance model parameters, and $Y(\theta, t_i)$ is the *ith* predicted value from the pharmacokinetic model. The goodness-of-fit was assessed by visual inspection, system convergence, Akaike Information Criterion, estimator criterion value for the maximum likelihood method, and examination of residuals.

RESULTS

The nonliposomal PBPK model was used to simulate tissue distribution of AmB following single and multiple dose administration of Fungizone® to mice. In general, reasonable prediction of tissue concentration-time profiles were obtained (Fig. 2), with the exception of the lung tissue for which the concentrations were slightly overpredicted. Therefore, the partition coefficient for the lung nonliposomal compartment was allowed to be estimated in the final dual PBPK model.

The initial estimation of the AmB release kinetics from liposomes was performed using the model structure shown in Figure S1. Plasma concentration-time profiles of AmB following administration of Fungizone® to rats and humans are shown in Fig. 3a and b. A two-compartment model provided a good description of the observed data. Parameters estimated for Fungizone®

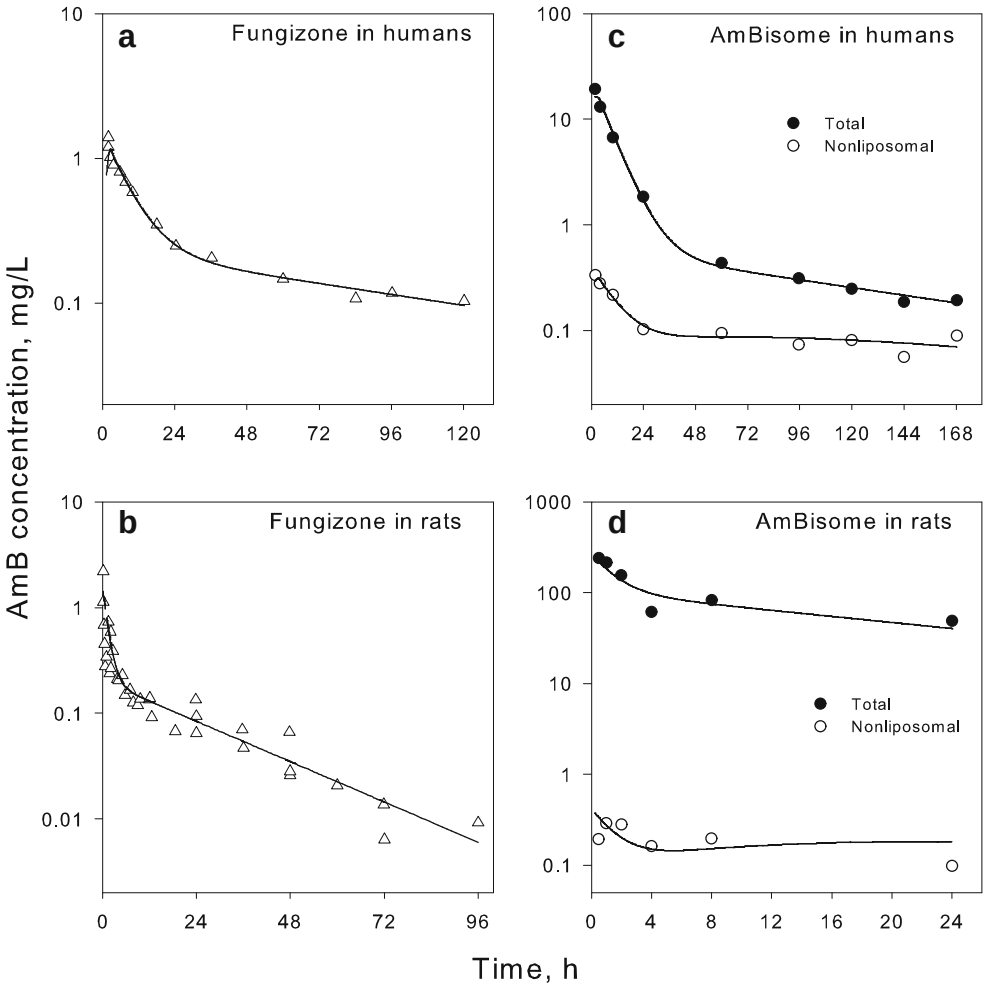

Fig. 3 Time-course of plasma AmB in rats and humans following single IV bolus administration of Fungizone® and AmBisome®. *Symbols* represent data extracted from references (Δ—Fungizone in humans (43) and rats (6,34,35); ○—nonliposomal AmB, ●—total AmB for AmBisome® in humans (24) and rats (27)). Lines are model fitted profiles using a compartmental model (Figure S1).

disposition (Online supplement, Table S2) were fixed and further utilized for fitting a compartmental model to AmBisome® data. The first-order rate constant of AmB release from liposomes was estimated to be 0.0035 h^{-1} in both species. Figures 3c and d show the total and nonliposomal plasma pharmacokinetic profiles of AmB following administration of AmBisome® to rats and humans. The simple model structure (Figure S1) allowed for a reasonable description of the data and parameters were estimated with good precision (Table-S2). A fraction of the dose that undergoes rapid release was estimated to be approximately 2 and 8% for rats and humans. The exact mechanism of this rapid release is unknown, and *in vitro* studies might be required for a more complete assessment of the release kinetics.

The dual PBPK model (Fig. 1) was used to characterize total concentrations of AmB in tissue and plasma following AmBisome® administration. However, the initial model structure that included linear uptake clearances for liposomes in all organs did not fit well (data not shown). To improve model performance, a saturable mechanism for liposomal uptake into the major organs of the RES system (liver and spleen) was incorporated into the model. Saturable uptake of liposomes into the liver was previously described for AmBisome® in an *ex-vivo* system (33). The final model resulted in a good simultaneous description of the data from mouse and rat studies and from several different administration regimens (Figs. 4 and 5). The corresponding pharmacokinetic parameters were estimated with sufficient precision (Table II). In the final model, the uptake clearance for liposomes was included for liver, spleen, GI tract, and remainder compartments. The values of uptake clearances for other organs were estimated to be very small during preliminary model runs and were fixed to zero in the final model.

To evaluate the predictive performance of the dual PBPK model for human AmB pharmacokinetics, drug exposure in different tissues following administration of AmBisome® was simulated. The resulting concentration-time profiles were visually compared to published data. Several theoretical allometric exponents (0.67, 0.75, 1) were evaluated for scaling the uptake clearance for liposomal compartments in tissues. The best predictive performance was obtained using an allometric exponent of 0.75. Figure 6 shows total and nonliposomal concentration-time profiles of AmB in plasma after single 2-h intravenous infusion of AmBisome® (2 mg/kg). The model reasonably predicted the pharmacokinetic profile of total AmB, including the maximal plasma concentration and terminal half-life. For the nonliposomal profile, model predictions were within a 2-fold range for most time points but missed the trend of the alpha phase. Interestingly, the simulated tissue concentration-time profiles following multiple AmBisome® administration were in good agreement with autopsy data (Fig. 7).

DISCUSSION

Incorporation of a drug into particulate carriers (e.g., liposomes) can improve drug solubility profiles, prolong circulation half-lives, and facilitate targeted delivery to the site of action, thereby enhancing efficacy and reducing toxicity. These advantages often come at the expense of more complex pharmacokinetics, which is controlled by a combination of properties of the drug molecule itself and the delivery system. Whereas measuring drug concentration in blood is relatively straightforward, the corresponding concentration in target tissues (site of action) is experimentally challenging in humans. Prediction of concentration-time profiles in target tissues in humans is essential for establishing pharmacokinetic-pharmacodynamic relationships for drugs with primary site of actions within specific tissues (such as AmB). PBPK modeling is particularly suitable for this purpose. Utilization of the PBPK modeling framework in combination with allometric principles allows for effective sharing of model structure and parameters among species. Combining information from mouse and rat studies was required for building the AmB dual PBPK model. The disposition parameters for nonliposomal AmB were based on Fungizone® pharmacokinetics in rats (6,25, 34,35); and very few studies have evaluated AmBisome® pharmacokinetics in this species (27). Most pharmacokinetic (and pharmacodynamic) studies of AmBisome® have been performed in mice (Table I).

Saturation of particle uptake by the organs of the RES might result in dose-dependent pharmacokinetics (33,36). Such pharmacokinetic behavior is frequently described using a Michaelis-Menten type function, in which the saturation is driven by relatively high drug concentrations in the plasma. However, an alternative mechanism, based on the saturation of the "tissue" compartment, might provide a more physiological description of the saturable kinetics of phagocytic processes (the cellular capacity for uptake of particles) (29,30). A combination of two saturable clearance pathways was used to mathematically describe hepatic uptake of liposomal AmB in isolated perfused liver experiments in rats. Due to the relatively short time-span of the perfusion experiments, efflux from the liver was assumed to be negligible and only the accumulation of AmB was incorporated (33). Our final PBPK model (Fig. 1) included this non-Michaelis-Menten mechanism into the structure of the liver and spleen liposomal compartments, which was necessary for simultaneous description of single and multiple doses of AmBisome® pharmacokinetics in mice. Owing to limited data, a combination of parallel uptake processes could not be identified.

Utilization of PBPK models for drug development and regulatory considerations is increasing (16); however, PBPK models for particulate formulations are limited (9,37). A simulation study for the optimization of liposomal doxorubicin utilized a semi-physiological model that included a separate tumor tissue compartment (38). The elimination of liposome was mediated through the uptake to a RES compartment and drug release

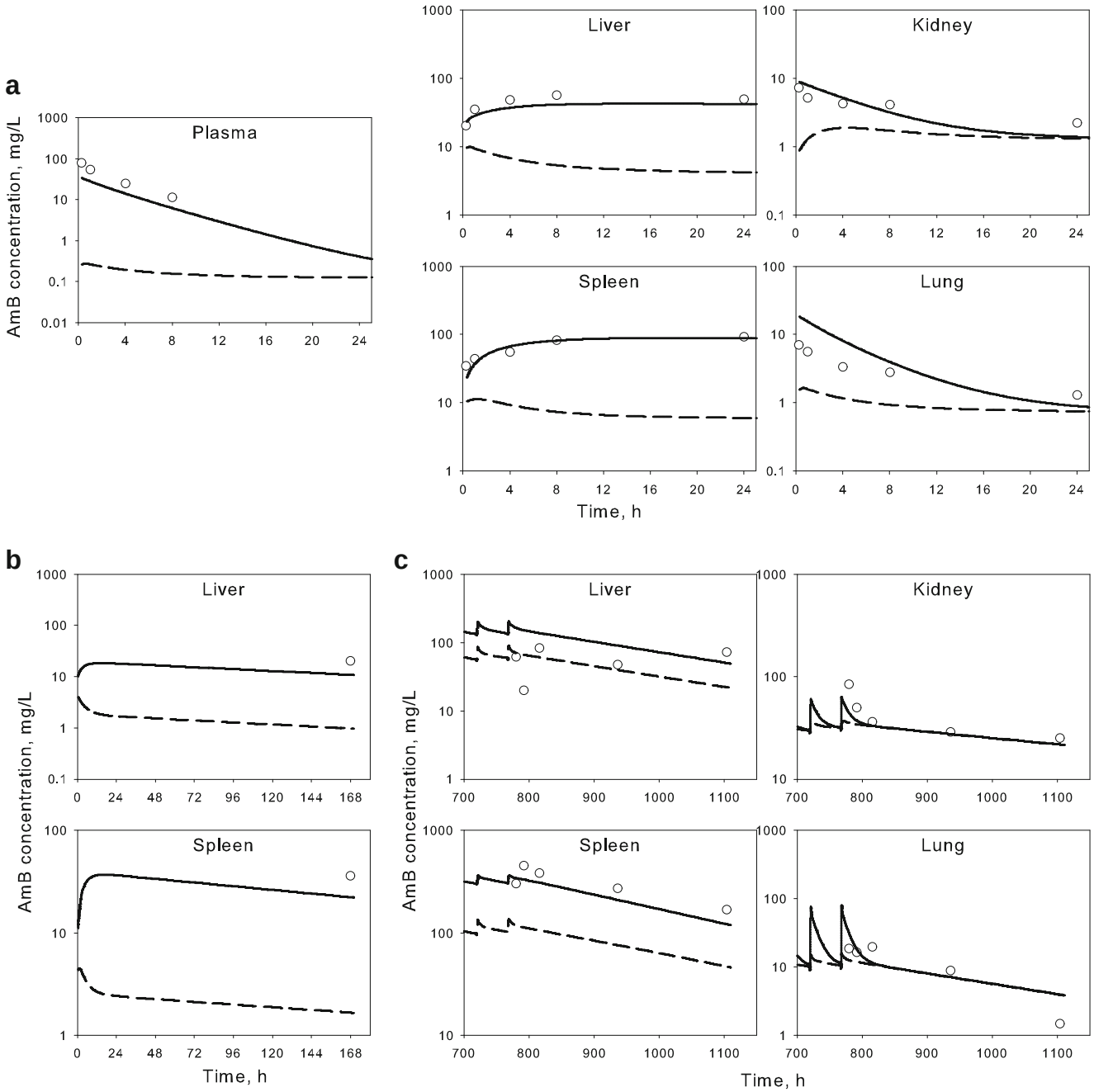

Fig. 4 Time-course of AmB in plasma and different tissues of mice following single and multiple IV bolus administration of AmBisome. *Symbols* represent total observed AmB concentrations and *solid lines* are model predicted profiles after simultaneous fitting of mouse and rat data using dual PBPK model. *Dashed lines* represent the corresponding model predicted nonliposomal concentrations. Observed data extracted from references: (**a**) Single 5 mg/kg dose (44); (**b**) Single 2 mg/kg dose (13). (**c**) 15 mg/kg dose three times a week for 5 weeks (45).

was allowed to occur in both blood and tumor compartments. However, the release of the drug from liposomes within the RES system and the return of the released drug to the systemic circulation were not considered. In our dual PBPK model, it was assumed that AmB can undergo elimination only in nonliposomal form, and the release from liposomes was assumed to occur in all compartments with the same rate constant. A previous comparison of AmB pharmacokinetics in humans following administration of liposomal and deoxycholate formulations also suggested that renal and fecal excretion of AmB occurs following the release of AmB from liposomes (24).

Interspecies differences in the pharmacokinetics of liposomal formulations have not been sufficiently characterized, and prediction of the human pharmacokinetic and pharmacodynamic

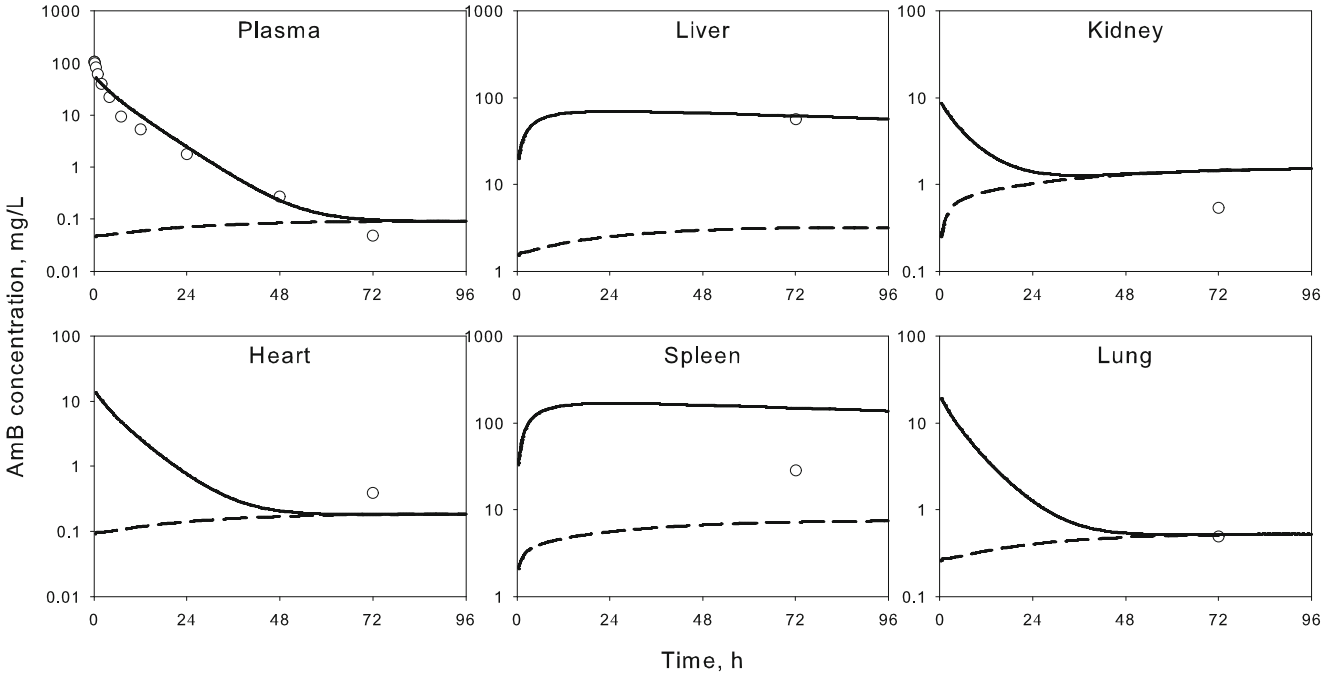

Fig. 5 Time-course of AmB in plasma and different tissues of rats following single IV bolus administration of AmBisome® (5 mg/kg). *Symbols* represent total observed AmB concentrations and *solid lines* are model predicted profiles after simultaneous fitting of mouse and rat data using dual PBPK model. *Dashed lines* represent the corresponding model predicted nonliposomal concentrations. Observed data extracted from references (6).

properties for particulate formulations remains a complex task (11). Liposomes with the same lipid composition exhibit different circulation half-lives in different species and the mechanism of liver uptake is species-specific (39). In rats, the hepatic uptake of liposomes is dependent on serum opsonins, whereas in mice no such dependency exists. In addition, the activity of serum opsonins differed among animal species (39). Species differences in liposome clearance (among mice, rats, and rabbits) appear to result from the uptake ability of the Kupffer cells in the liver, and not from the differences in the density of these cells among species (12). Recently, Caron and coworkers evaluated allometric scaling approaches for pegylated liposomal anticancer drugs (i.e., doxorubicin and cisplatin). Human clearance could not be predicted from preclinical data, despite a strong correlation between body weight and the variables of the mononuclear phagocyte system (40). PBPK modeling allows for a more mechanistic description of distribution and elimination processes, and might provide a better approach for predicting human pharmacokinetics of particulate formulations. During PBPK

Table II Estimated Pharmacokinetic Parameters of AmB in Mice using the Final Dual PBPK Model

Parameter	Units	Estimate	%CV
K_{lu}		6.00	19
Up_{gi}	L/h	$2.04 \cdot 10^{-4}$	15
Up_{sp}	L/h	$5.95 \cdot 10^{-5}$	20
Up_{li}	L/h	$4.62 \cdot 10^{-4}$	21
Up_{rm}	L/h	$1.97 \cdot 10^{-5}$	50
Up_{lu}	L/h	0	–[a]
Up_{kd}	L/h	0	–[a]
C_{sp}^{MAX}	mg/L	270	18
C_{li}^{MAX}	mg/L	121	21
FR_{mouse}		0.179	28
FR_{rat}		1.83	–[a]
FR_{human}		8.16	–[a]

[a] fixed value

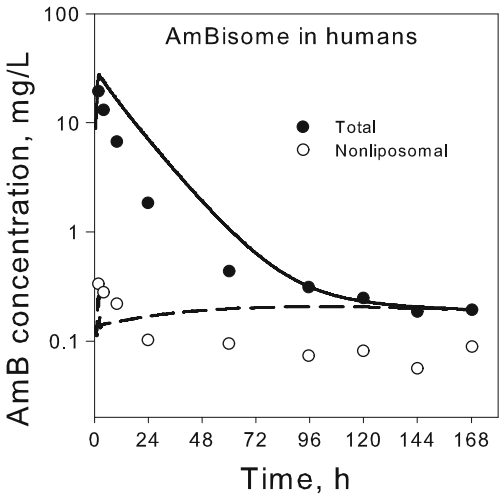

Fig. 6 Time-course of plasma AmB concentrations in humans following single IV administration of AmBisome. *Symbols* represent data extracted from reference (24); ○—nonliposomal AmB, ●—total AmB. Lines are model predicted profiles simulated by dual PBPK model using scaling approach described in the text; *dashed line* nonliposomal AmB, solid line—total AmB.

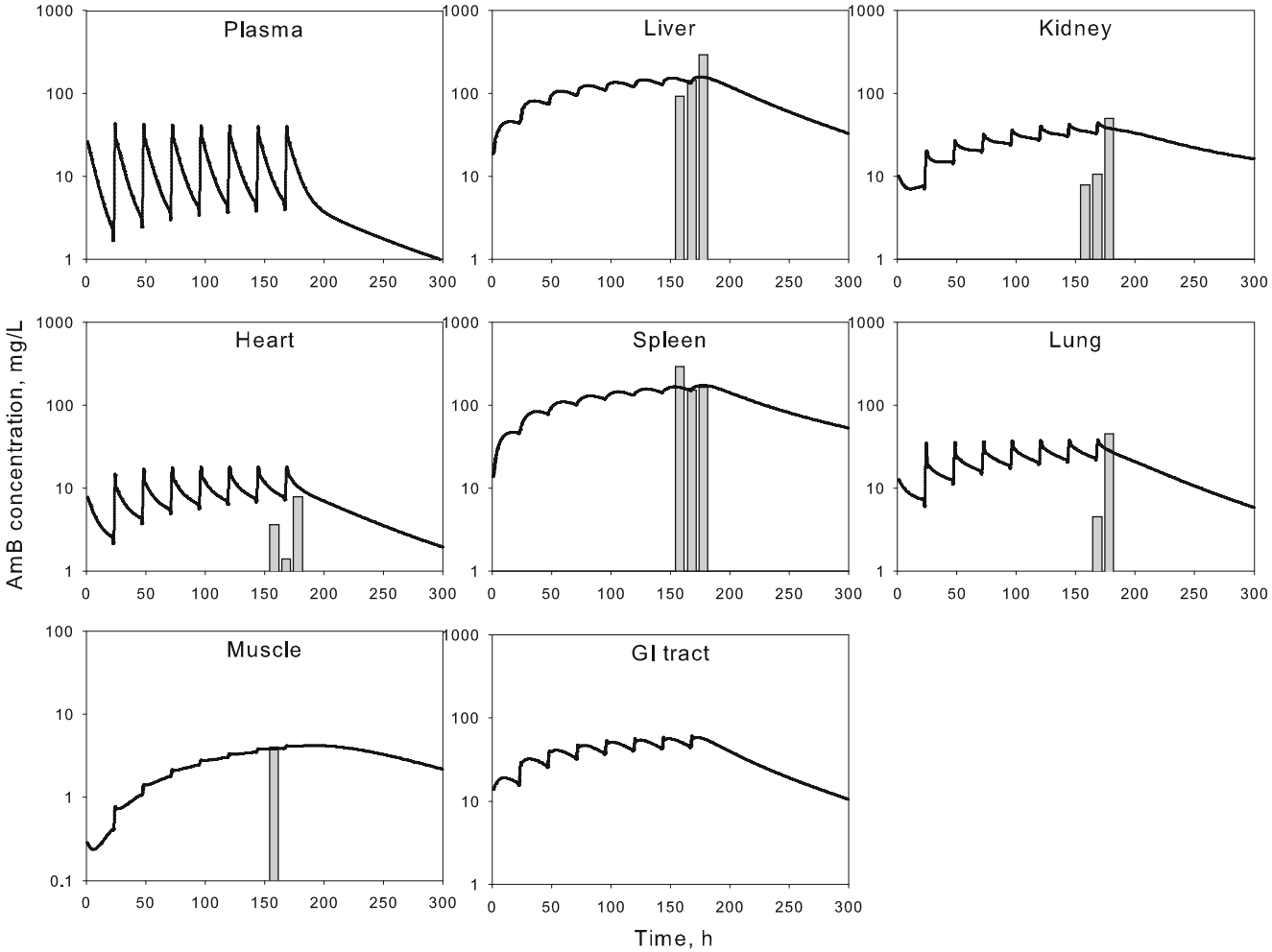

Fig. 7 Time-course of plasma and tissue AmB concentrations in humans following multiple IV bolus administration of AmBisome. Solid lines are total AmB concentrations (2.2 mg/kg of AmBisome® per day for 7 days) predicted by dual PBPK model using simulation and scaling approach described in the text. *Bars* represent observed human tissue concentrations as reported in (31,32) after multiple administration of a median dose of 2.2 mg/kg (exact dosing and patient information and sampling time were not reported). For muscle tissue, line represents concentration in the remainder compartment.

model development, allometric expressions were incorporated to allow for simultaneous description of the pharmacokinetic data from different species. Scaling of the parameters for nonliposomal drug was based on previously published models (28) and has been shown to provide a good prediction of AmB pharmacokinetics in humans (following administration of deoxycholate formulation) based on animal data (17). Since interspecies differences in uptake kinetics of liposomes containing AmB are unknown, a range of allometric exponents for uptake clearance was evaluated. The best prediction of human data was obtained by scaling the uptake clearance with an allometric exponent of 0.75. Further investigation of the molecular determinants of particle uptake to the RES is required for better understanding of the species difference and appropriate scaling methods for this process.

The data used in this analysis were collected from multiple publications, as no single study contained sufficient information for developing a dual PBPK model. The influence of potential differences in the experimental settings (including bioanalytical assays) and the variability within the studies remain unknown and could not be further evaluated with the model. Several tissue pharmacokinetic profiles contain few data points, which might contribute to some bias in parameter estimates. Future studies, evaluating these and other study limitations may facilitate the further optimization of the model.

In conclusion, a dual PBPK model successfully described plasma and tissue pharmacokinetics of AmB after administration of AmBisome® to rats and mice. The final model demonstrated good predictive performance by reasonably simulating AmB exposure in human tissues. Since treatment success is dependent on the concentration of AmB in target tissues, it is critical to predict drug exposure in human tissues following different routes of administration. This modeling framework can be potentially utilized for optimizing AmBisome® therapy in humans and for investigating pathophysiological factors controlling AmB pharmacokinetics and pharmacodynamics.

REFERENCES

1. Thornton SJ, Wasan KM. The reformulation of amphotericin B for oral administration to treat systemic fungal infections and visceral leishmaniasis. Expert Opin Drug Deliv. 2009;6(3):271–84.
2. Thornton SJ, Wasan KM, Piecuch A, Lynd LL, Wasan EK. Barriers to treatment for visceral leishmaniasis in hyperendemic areas: India, Bangladesh, Nepal, Brazil and Sudan. Drug Dev Ind Pharm. 2010;36(11):1312–9.
3. Adler-Moore J, Proffitt RT. Am Bisome: liposomal formulation, structure, mechanism of action and pre-clinical experience. J Antimicrob Chemother. 2002;49 Suppl 1:21–30.
4. Bern C, Adler-Moore J, Berenguer J, Boelaert M, den Boer M, Davidson RN, *et al.* Liposomal amphotericin B for the treatment of visceral leishmaniasis. Clin Infect Dis Off Publ Infect Dis Soc Am. 2006;43(7):917–24.
5. Amidon GL, Lennernas H, Shah VP, Crison JR. A theoretical basis for a biopharmaceutic drug classification: the correlation of in vitro drug product dissolution and in vivo bioavailability. Pharm Res. 1995;12(3):413–20.
6. Gershkovich P, Wasan EK, Lin M, Sivak O, Leon CG, Clement JG, *et al.* Pharmacokinetics and biodistribution of amphotericin B in rats following oral administration in a novel lipid-based formulation. J Antimicrob Chemother. 2009;64(1):101–8.
7. Davidson EM, Barenholz Y, Cohen R, Haroutiunian S, Kagan L, Ginosar Y. High-dose bupivacaine remotely loaded into multivesicular liposomes demonstrates slow drug release without systemic toxic plasma concentrations after subcutaneous administration in humans. Anesth Analg. 2010;110(4):1018–23.
8. Adler-Moore JP, Proffitt RT. Amphotericin B lipid preparations: what are the differences? Clinical Microbiol Infect Off Publ Eur Soc Clin Microbiol Infect Dis. 2008;14 Suppl 4:25–36.
9. Landsiedel R, Fabian E, Ma-Hock L, Wohlleben W, Wiench K, Oesch F, et al. Toxico-/biokinetics of nanomaterials. Archives of toxicology. 2012.
10. Li SD, Huang L. Pharmacokinetics and biodistribution of nanoparticles. Mol Pharm. 2008;5(4):496–504.
11. Martinez MN. Factors influencing the use and interpretation of animal models in the development of parenteral drug delivery systems. AAPS J. 2011;13(4):632–49.
12. Harashima H, Komatsu S, Kojima S, Yanagi C, Morioka Y, Naito M, *et al.* Species difference in the disposition of liposomes among mice, rats, and rabbits: allometric relationship and species dependent hepatic uptake mechanism. Pharm Res. 1996;13(7):1049–54.
13. Gershkovich P, Wasan EK, Sivak O, Li R, Zhu X, Werbovetz KA, et al. Visceral leishmaniasis affects liver and spleen concentrations of amphotericin B following administration to mice. J Antimicrob Chemother. 2009.
14. Benson JM, Nahata MC. Pharmacokinetics of amphotericin B in children. Antimicrob Agents Chemother. 1989;33(11):1989–93.
15. Graybill JR. Is there a correlation between serum antifungal drug concentration and clinical outcome? J Infect. 1994;28 Suppl 1:17–24.
16. Rowland M, Peck C, Tucker G. Physiologically-based pharmacokinetics in drug development and regulatory science. Annu Rev Pharmacol Toxicol. 2011;51:45–73.
17. Kagan L, Gershkovich P, Wasan KM, Mager DE. Physiologically based pharmacokinetic model of amphotericin B disposition in rats following administration of deoxycholate formulation (Fungizone®): pooled analysis of published data. AAPS J. 2011;13(2):255–64.
18. Brown RP, Delp MD, Lindstedt SL, Rhomberg LR, Beliles RP. Physiological parameter values for physiologically based pharmacokinetic models. Toxicol Ind Health. 1997;13(4):407–84.
19. Davies B, Morris T. Physiological parameters in laboratory animals and humans. Pharm Res. 1993;10(7):1093–5.
20. Gerlowski LE, Jain RK. Physiologically based pharmacokinetic modeling: principles and applications. J Pharm Sci. 1983;72(10):1103–27.
21. Tsuji A, Yoshikawa T, Nishide K, Minami H, Kimura M, Nakashima E, *et al.* Physiologically based pharmacokinetic model for beta-lactam antibiotics I: tissue distribution and elimination in rats. J Pharm Sci. 1983;72(11):1239–52.
22. Gibaldi M, Perrier D. Pharmacokinetics. 2nd ed. New York: Marcel Dekker, Inc.; 1982.
23. Robbie G, Chiou WL. Elucidation of human amphotericin B pharmacokinetics: identification of a new potential factor affecting interspecies pharmacokinetic scaling. Pharm Res. 1998;15(10):1630–6.
24. Bekersky I, Fielding RM, Dressler DE, Lee JW, Buell DN, Walsh TJ. Plasma protein binding of amphotericin B and pharmacokinetics of bound versus unbound amphotericin B after administration of intravenous liposomal amphotericin B (AmBisome) and amphotericin B deoxycholate. Antimicrob Agents Chemother. 2002;46(3):834–40.
25. Wang LH, Fielding RM, Smith PC, Guo LS. Comparative tissue distribution and elimination of amphotericin B colloidal dispersion (Amphocil) and Fungizone after repeated dosing in rats. Pharm Res. 1995;12(2):275–83.
26. Chow HH, Wu Y, Mayersohn M. Pharmacokinetics of amphotericin B in rats as a function of dose following constant-rate intravenous infusion. Biopharm Drug Dispos. 1995;16(6):461–73.
27. Matsui S, Imai S, Yabuki M, Komuro S. Pharmacokinetics characterization of liposomal amphotericin B: investigation of clearance process and drug interaction potential. Arzneimittelforschung. 2009;59(9):461–70.
28. Kawai R, Lemaire M, Steimer JL, Bruelisauer A, Niederberger W, Rowland M. Physiologically based pharmacokinetic study on a cyclosporin derivative, SDZ IMM 125. J Pharmacokinet Biopharm. 1994;22(5):327–65.
29. Harashima H, Kume Y, Yamane C, Kiwada H. Non-michaelismenten type hepatic-uptake of liposomes in the rat. J Pharm Pharmacol. 1992;44(9):707–12.
30. Kume Y, Maeda F, Harashima H, Kiwada H. Saturable, non-Michaelis-Menten uptake of liposomes by the reticuloendothelial system. J Pharm Pharmacol. 1991;43(3):162–6.
31. Tollemar J, Ringden O, Tyden G. Liposomal amphotericin-B (Ambisome) treatment in solid organ and bone-marrow transplant recipients—efficacy and safety evaluation. Clin Transplant. 1990;4(3):167–75.
32. Ringden O, Meunier F, Tollemar J, Ricci P, Tura S, Kuse E, *et al.* Efficacy of amphotericin B encapsulated in liposomes (AmBisome) in the treatment of invasive fungal infections in immunocompromised patients. J Antimicrob Chemother. 1991;28(Suppl B):73–82.
33. Hong Y, Ramzan I, McLachlan AJ. Disposition of amphotericin B in the isolated perfused rat liver. J Pharm Pharmacol. 2004;56(1):35–41.
34. Angra PK, Siddig A, Nettey H, Desai N, Oettinger C, D'Souza MJ. Pharmacokinetic and biodistribution studies of amphotericin B microspheres. J Microencapsul. 2009;26(7):627–34.
35. Fielding RM, Smith PC, Wang LH, Porter J, Guo LS. Comparative pharmacokinetics of amphotericin B after administration of a novel colloidal delivery system, ABCD, and a conventional formulation to rats. Antimicrob Agents Chemother. 1991;35(6):1208–13.
36. Chow DD, Essien HE, Padki MM, Hwang KJ. Targeting small unilamellar liposomes to hepatic parenchymal cells by dose effect. J Pharmacol Exp Ther. 1989;248(2):506–13.
37. Li M, Al-Jamal KT, Kostarelos K, Reineke J. Physiologically based pharmacokinetic modeling of nanoparticles. ACS nano. 2010;4(11):6303–17.
38. Harashima H, Iida S, Urakami Y, Tsuchihashi M, Kiwada H. Optimization of antitumor effect of liposomally encapsulated doxorubicin based on simulations by pharmacokinetic/pharmacodynamic modeling. J control Rel Off J Control Rel Soc. 1999;61(1–2):93–106.

39. Liu D, Hu Q, Song YK. Liposome clearance from blood: different animal species have different mechanisms. Biochim Biophys Acta. 1995;1240(2):277–84.
40. Caron WP, Clewell H, Dedrick R, Ramanathan RK, Davis WL, Yu N, *et al.* Allometric scaling of pegylated liposomal anticancer drugs. J Pharmacokinet Pharmacodyn. 2011;38(5):653–69.
41. van Etten EW, Otte-Lambillion M, van Vianen W, ten Kate MT, Bakker-Woudenberg AJ. Biodistribution of liposomal amphotericin B (AmBisome) and amphotericin B-desoxycholate (Fungizone) in uninfected immunocompetent mice and leucopenic mice infected with Candida albicans. J Antimicrob Chemother. 1995;35(4):509–19.
42. Sivak O, Gershkovich P, Lin M, Wasan EK, Zhao J, Owen D, *et al.* Tropically stable novel oral lipid formulation of amphotericin B (iCo-010): biodistribution and toxicity in a mouse model. Lipids Health Dis. 2011;10:135.
43. Bekersky I, Fielding RM, Dressler DE, Lee JW, Buell DN, Walsh TJ. Pharmacokinetics, excretion, and mass balance of liposomal amphotericin B (AmBisome) and amphotericin B deoxycholate in humans. Antimicrob Agents Chemother. 2002;46(3):828–33.
44. Proffitt RT, Satorius A, Chiang SM, Sullivan L, Adler-Moore JP. Pharmacology and toxicology of a liposomal formulation of amphotericin B (AmBisome) in rodents. J Antimicrob Chemother. 1991;28(Suppl B):49–61.
45. Smith PJ, Olson JA, Constable D, Schwartz J, Proffitt RT, Adler-Moore JP. Effects of dosing regimen on accumulation, retention and prophylactic efficacy of liposomal amphotericin B. J Antimicrob Chemother. 2007;59(5):941–51.